Arabian Journal of Chemistry (2022) **15**, 103560

King Saud University

Arabian Journal of Chemistry

www.ksu.edu.sa
www.sciencedirect.com

ORIGINAL ARTICLE

Ionic liquid mediated four-component synthesis of novel phthalazinone based indole-pyran hybrids as cytotoxic agents

M. Shaheer Malik [a,*], Reem I. Alsantali [b], Meshari A. Alsharif [a], Sultan I. Aljayzani [a], Moataz Morad [a], Rabab S. Jassas [c], Munirah M. Al-Rooqi [a], Abdulrahman A. Alsimaree [d], Hatem M. Altass [a], Basim H. Asghar [a], Abdelrahman S. Khder [a,e], Saleh A. Ahmed [a,f,*]

[a] *Department of Chemistry, Faculty of Applied Sciences, Umm Al-Qura University, Makkah 21955, Saudi Arabia*
[b] *Department of Pharmaceutical Chemistry, College of Pharmacy, Taif University, P.O. Box 11099, Taif 21944, Saudi Arabia*
[c] *Department of Chemistry, Jamoum University College, Umm Al-Qura University, 21955 Makkah, Saudi Arabia*
[d] *Department of Basic Science (Chemistry), College of Science and Humanities, Shaqra University, Afif, Saudi Arabia*
[e] *Faculty of Science, Chemistry Department, Mansoura University, 35516 Mansoura, Egypt*
[f] *Department of Chemistry, Faculty of Science, Assiut University, 71516 Assiut, Egypt*

Received 29 August 2021; accepted 8 November 2021
Available online 12 November 2021

KEYWORDS

Phthalazine;
Indole;
Ionic liquids;
Multicomponent reaction;
Anticancer activity;
Molecular docking;
Computational analysis

Abstract A robust design and synthesis of novel phthalazinone based indole-pyran hybrids as cytotoxic agents is described. A relatively safer ionic liquid medium ([BMIM]BF_4) was utilized to mediate a one-pot, four-component reaction to access the novel hybrids in short reaction time and good yields. The cytotoxic potential of the hybrids was investigated against selected cancer cell lines. The hybrids **5h** and **5b** displayed potent activity with IC_{50} values in the range of 5.8–9.6 μM. The insilico docking demonstrated a pronounced affinity of hybrids **5h** and **5b** towards the human tankyrase-1 enzyme exhibiting binding energies values of −11.2 and −10.2 kcal/mole, respectively. Additional ADME and drug likeliness analyses revealed the potential of the active hybrids to be taken forward for advanced studies.

* Corresponding authors at: Department of Chemistry, Faculty of Applied Sciences, Umm Al-Qura University, Makkah 21955, Saudi Arabia
E-mail addresses: msmalik@uqu.edu.sa (M.S. Malik), saahmed@uqu.edu.sa (S.A. Ahmed).

Peer review under responsibility of King Saud University.

Production and hosting by Elsevier

https://doi.org/10.1016/j.arabjc.2021.103560
1878-5352

1. Introduction

In the post-genomic era, heterocyclic scaffolds have emerged as the crux of modern drug discovery programs. Heterocyclic scaffolds provide ample opportunity to alter different physicochemical properties of an active agent, thereby modulating its ADMET properties (Jampilek 2019). The heterocyclic systems such as indole, phthalazine, and annulated pyrans are classified as privileged structures because they are capable of binding at different biological target receptors. Phthalazine is a unique scaffold that possesses various therapeutic applications such as anticancer, cardiotonic, antibacterial, vasorelaxant, and antidiabetics (Sangshetti et al., 2019, Zaib and Khan 2020). Recently, phthalazinones have emerged as effective therapeutic pharmacophores in the area of anticancer drug design (Vila et al., 2015). The phthalazinone moiety is a core unit in olaparib, and talazoparib, which are poly (ADP-ribose) polymerase (PARP) inhibitors approved by US Food and Drug Administration (Fig. 1). They are clinically used in the treatment of ovarian and metastatic breast cancers (Boussios et al., 2020, Arora et al., 2021).

Similarly, indole is a bicyclic heterocyclic molecule widely distributed in naturally occurring compounds (Gul and Hamann 2005, Singh and Singh 2018). It is considered a promising molecule in drug discovery and development due to its vast applications in medicinal chemistry. Most of the indole containing compounds exhibits various therapeutic applications like antimicrobial, anti-inflammatory, antihistamine, antioxidant, antidiabetic, antiviral, and anticancer properties (Kumari and Singh 2019). The indole moiety is widely used in anticancer drug discovery and several indole derivatives such as midostaurin, rucaparib, panobinostat, etc., are FDA-approved anticancer drugs (Garnock-Jones 2015, Shirley 2019, Sly and Gaspar 2019). The indole-based compound exerts the cytotoxic potency by modulating different biological receptors, which includes histone deacetylases, tubulin polymerization, enzymes associated with DNA, sirtuins and kinases (Dadashpour and Emami 2018). Interestingly, the pyran moiety are also well-documented in the design of new pharmaceutical agents (Kumar et al., 2017). Moreover, the functionalities such as cyano, amino and ethoxycarbonyl groups are known to modulate the properties of pharmacophores. They are present in many drugs marketed and used for diverse indications (Fleming et al., 2010, Walker et al., 2010).

The development of new chemical methodologies with environmentally friendlier aspects is a pressing need because of the adverse environmental degradation associated with pure chemical processes. In this direction, the use of multicomponent reactions and ionic liquids renders a chemical process greener and environmentally benign compared to the use of two-component reactions in volatile organic solvents. The primary advantage of multicomponent reaction is the conservation of atom economy, a guiding principles in green chemistry, in addition to some other benefits (Cioc et al., 2014). On the other hand, ionic liquids (ILs), with an organic cation, have attracted much consideration as a relatively greener solvent due to their superior physical and electronic properties (Lei et al., 2017, Vekariya 2017). However, the ionic liquids were not cost-effective with apprehension about toxicity, which led to the exploration of more sustainable alternatives. In the recent past, 1-butyl-3-methyl imidazolium-based ionic liquids have drawn significant attention as comparatively safer media in various organic transformations such as hydrogenations, Heck reaction, Bischler-Napieralski reaction (Vekariya 2017). Further, a more benign IL, 1-butyl-3-methyl imidazolium

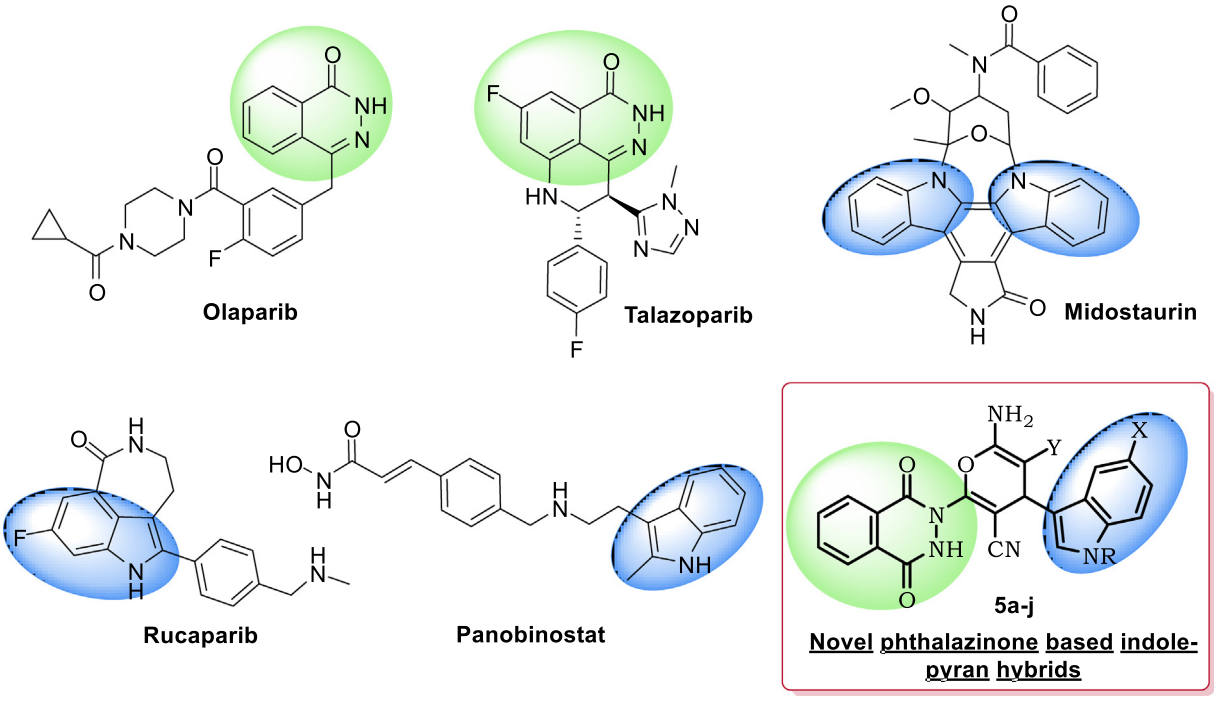

Fig. 1 Anticancer agents with phthalazinone and indole moieties.

tetrafluoroborate ([BMIM]BF_4), was successfully applied in different organic conversions to access bioactive heterocycles (Banerjee 2017).

Considering the significance of indole and phthalazinone scaffolds in anticancer drug discovery, we have designed and synthesized novel phthalazinone based indole-pyran hybrids through a multicomponent reaction in ionic liquid. This endeavor continued our previous research on the development of new bioactive molecules and synthetic methodologies (Shaheer Malik et al., 2020, Malik et al., 2021). Our newly developed method employs an environmentally safer one-pot four-component reaction promoted by the ionic liquid, [BMIM]BF_4. The synthesized new phthalazinone based indole-pyran hybrids were tested to recognize their cytotoxic potential against some selected cancer cell lines. The active hybrids were subjected to molecular docking to recognize their binding affinity at the biological receptor active site. In addition to this, other computational studies were also undertaken to understand the molecular descriptors and drug likeliness properties of the hybrids.

2. Experimental

2.1. Chemistry: General procedure for the synthesis of novel phthalazinone based indole-pyran hybrids 5a-j

Dimethyl phthalate **1** (1 eq, 1.94 g, 10 mmol), cyanoacetohydrazide **2** (1 eq, 0.99 g, 10 mmol), 1H-indole-3-carbaldehydes **3** (1 eq, 10 mmol) and malononitrile (1 eq, 0.66 g, 10 mmol)/ ethyl 2-cyanoacetate **4a-4b** (1 eq, 1.13 g, 10 mmol) were added into [BMIM]BF_4 (8 eq, 18.08 g, 80 mmol) and heated at 75–80 °C for 60–120 min. Thin layer chromatography was employed to monitor the course of the reaction. After the reaction is complete, the reaction mass was brought to room temperature and cold water was added. The resulting mixture was stirred for 30 min and the crude solid was separated by filtration followed by recrystallization from ethanol solvent. The recrystallized solid was dried at 60–65 °C overnight to afford pure novel phthalazinone based indole-pyran hybrids **5a-j**.

2.2. 2-Amino-6-(1,4-dioxo-3,4-dihydrophthalazin-2(1H)-yl)-4-(1H-indol-3-yl)-4H-pyran-3,5-dicarbonitrile 5a

Yield: 85 %; IR (KBr) cm^{-1}: 3385 (broad, —NH), 2189 (—CN), 1644 (C═O); ^{1}H NMR (DMSO d_6, 400 MHz): δ 4.8 (s, 1H, —CH), δ 7.0–8.2 (m, 11*H*, Ar-H, and NH_2), δ 11.5 (s, 1H, —NH), δ 12.2 (s, 1H, —NH); ^{13}C NMR (DMSO d_6, 100 MHz): δ 43.1, 52.5, 63.2, 111.8, 114.1, 115.6, 115.9, 116.6, 122.5, 124.0, 127.2, 127.7, 128.2, 128.3, 135.5, 146.2, 153.4, 155.3, 160.5, 162.2, 166.2 172.2, 177.2; [M + H^+]: 423.

2.3. 2-Amino-6-(1,4-dioxo-3,4-dihydrophthalazin-2(1H)-yl)-4-(1-methyl-1H-indol-3-yl)-4H-pyran-3,5-dicarbonitrile 5b

Yield: 84 %; IR (KBr) cm^{-1}: 3405 (broad, —NH), 2187 (—CN), 1658 (C═O); ^{1}H NMR (DMSO d_6, 400 MHz): δ 3.6 (s, 3H, —CH_3), δ 4.8 (s, 1H, —CH), δ 7.0–8.3 (m, 11*H*, Ar-H, and NH_2), δ 11.4 (s, 1H, —NH); ^{13}C NMR (DMSO d_6, 100 MHz): δ 34.1, 43.1, 52.2, 63.1, 110.9, 114.1, 116.0, 118.6, 119.1, 120.7, 122.3, 124.1, 125.1, 127.4, 128.2, 128.3, 139.2, 146.2, 148.4, 153.4, 163.2, 166.8, 172.0, 177.2; [M + H^+]: 436.

2.4. 2-Amino-6-(1,4-dioxo-3,4-dihydrophthalazin-2(1H)-yl)-4-(1-ethyl-1H-indol-3-yl)-4H-pyran-3,5-dicarbonitrile 5c

Yield: 83 %; IR (KBr) cm^{-1}: 3408 (broad, —NH), 2188 (—CN), 1659 (C═O); ^{1}H NMR (DMSO d_6, 400 MHz): δ 1.3 (t, 3H, —CH_3), 4.2 (q, 2H, —CH_2), δ 4.9 (s, 1H, —CH), δ 7.0–8.2 (m, 11*H*, Ar-H, and NH_2), δ 11.6 (s, 1H, —NH); ^{13}C NMR (DMSO d_6, 100 MHz): δ 12.2, 41.3, 43.2, 53.1, 64.2, 111.9, 115.2, 116.1, 118.7, 119.0, 120.8, 122.1, 123.2, 124.5, 127.6, 128.3, 128.4, 138.3, 145.3, 148.5, 153.3, 162.4, 166.7, 172.1, 177.3; [M + H^+]: 451.

2.5. 2-Amino-4-(5-chloro-1H-indol-3-yl)-6-(1,4-dioxo-3,4-dihydrophthalazin-2(1H)-yl)-4H-pyran-3,5-dicarbonitrile 5d

Yield: 81 %; IR (KBr) cm^{-1}: 3388 (broad, —NH), 2187 (—CN), 1654 (C═O); ^{1}H NMR (DMSO d_6, 400 MHz): δ 4.8 (s, 1H, —CH), δ 7.0–8.2 (m, 10*H*, Ar-H, and NH_2), δ 11.5 (s, 1H, —NH), δ 12.2 (s, 1H, —NH); ^{13}C NMR (DMSO d_6, 100 MHz): δ 42.3, 53.7, 63.2, 110.0, 111.4, 113.5, 114.8, 115.6, 121.3, 124.1, 128.1, 128.9, 129.2, 129.4, 135.6, 145.1, 152.3, 155.2, 161.4, 162.4, 171.3, 176.5; [M^+]: 456 and [M^{+2}]: 458.

2.6. 2-Amino-4-(5-bromo-1H-indol-3-yl)-6-(1,4-dioxo-3,4-dihydrophthalazin-2(1H)-yl)-4H-pyran-3,5-dicarbonitrile 5e

Yield: 81%; IR (KBr) cm^{-1}: 3382 (broad, —NH), 2182 (—CN), 1658 (C═O); ^{1}H NMR (DMSO d_6, 400 MHz): δ 4.7 (s, 1H, —CH), δ 7.1–8.2 (m, 10*H*, Ar-H, and NH_2), δ 11.6 (s, 1H, —NH), δ 12.1 (s, 1H, —NH); ^{13}C NMR (DMSO d_6, 100 MHz): δ 43.1, 52.8, 62.1, 111.1, 111.4, 114.6, 114.9, 115.9, 120.3, 123.2, 127.1, 128.8, 129.3, 129.9, 135.7, 145.2, 152.5, 155.5, 161.5, 162.8, 171.4, 176.6; [M^+]: 500 and [M^{+2}]: 502.

2.7. Ethyl 2-amino-5-cyano-6-(1,4-dioxo-3,4-dihydrophthalazin-2(1H)-yl)-4-(1H-indol-3-yl)-4H-pyran-3-carboxylate 5f

Yield: 83 %; IR (KBr) cm^{-1}: 3404 (broad, —NH), 1720 (C═O); ^{1}H NMR (DMSO d_6, 400 MHz): δ 1.3 (t, 3H, –CH_3), δ 4.3 (q, 2H, –CH_2), δ 4.9 (s, 1H, –CH), δ 6.8–7.9 (m, 11*H*, Ar-H, and NH_2), δ 11.5 (s, 1H, —NH), δ 12.1 (s, 1H, —NH); ^{13}C NMR (DMSO d_6, 400 MHz): δ 13.9, 43.1, 55.2, 61.5, 63.4, 111.8, 114.0, 114.2, 116.7, 122.5, 124.0, 127.3, 127.4, 127.7, 131.3, 146.3, 153.4, 155.3, 159.0, 165.7, 172.1, 177.2; [M + H^+]: 470.

2.8. Ethyl 2-amino-5-cyano-6-(1,4-dioxo-3,4-dihydrophthalazin-2(1H)-yl)-4-(1-methyl-1H-indol-3-yl)-4H-pyran-3-carboxylate 5g

Yield: 84 %; IR (KBr) cm^{-1}: 3411 (broad, —NH), 1716 (C═O); ^{1}H NMR (DMSO d_6, 400 MHz): δ 1.3 (t, 3H, —CH_3), δ 3.8 (s, 3H, —CH_3), δ 4.3 (q, 2H, —CH_2), δ 4.9 (s, 1H, —CH), δ 6.9–7.9 (m, 11*H*, Ar-H, and NH_2), δ 11.6 (s, 1H, —NH); ^{13}C NMR (DMSO d_6, 400 MHz): δ 14.1, 34.1, 41.4, 58.1, 62.5, 63.2, 111.0, 118.4, 119.1, 123.5, 124.1, 127.5,

128.6, 128.8, 133.2, 133.3, 142.1, 143.2, 145.0, 148.4, 152.5, 153.3, 158.1, 165.7, 172.0, 177.2; [M + H$^+$]: 484.

2.9. Ethyl 2-amino-5-cyano-6-(1,4-dioxo-3,4-dihydrophthalazin-2(1H)-yl)-4-(1-ethyl-1H-indol-3-yl)-4H-pyran-3-carboxylate 5h

Yield: 83 %; IR (KBr) cm^{-1}: 3422 (broad, —NH), 1700 (C═O); ^{1}H NMR (DMSO d_6, 400 MHz): δ 1.1 (t, 3H, —CH$_3$), δ 1.2 (t, 3H, —CH$_3$), δ 4.1 (q, 2H, —CH$_2$), δ 4.3 (q, 2H, —CH$_2$), δ 4.9 (s, 1H, —CH), δ 6.9–7.9 (m, 11*H*, Ar-H, and NH$_2$), δ 11.4 (s, 1H, —NH); ^{13}C NMR (DMSO d_6, 400 MHz): δ 14.0, 15.3, 41.2, 41.8, 58.2, 62.6, 64.2, 111.6, 118.6, 118.2, 123.6, 124.3, 126.6, 128.7, 128.9, 132.3, 133.2, 142.0, 143.3, 145.1, 148.3, 152.6, 153.6, 158.2, 164.6, 172.1, 177.3; [M + H$^+$]: 498.

2.10. Ethyl 2-amino-4-(5-chloro-1H-indol-3-yl)-5-cyano-6-(1,4-dioxo-3,4-dihydrophthalazin-2(1H)-yl)-4H-pyran-3-carboxylate 5i

Yield: 81 %; IR (KBr) cm^{-1}: 3410 (broad, —NH), 1701 (C═O); ^{1}H NMR (DMSO d_6, 400 MHz): δ 1.2 (t, 3H, —CH$_3$), δ 4.2 (q, 2H, —CH$_2$), δ 4.8 (s, 1H, —CH), δ 6.8–7.9 (m, 10*H*, Ar-H, and NH$_2$), δ 11.6 (s, 1H, —NH), δ 12.2 (s, 1H, —NH); ^{13}C NMR (DMSO d_6, 400 MHz): δ 14.2, 43.2, 54.2, 62.5, 63.6, 111.9, 114.1, 114.5, 116.8, 121.4, 124.1, 126.4, 127.5, 127.8, 131.5, 145.5, 153.5, 155.5, 159.1, 164.8, 172.3, 177.5; [M$^+$]: 503 and[M^{+2}]: 505.

2.11. Ethyl 2-amino-4-(5-bromo-1H-indol-3-yl)-5-cyano-6-(1,4-dioxo-3,4-dihydrophthalazin-2(1H)-yl)-4H-pyran-3-carboxylate 5j

Yield: 80 %; IR (KBr) cm^{-1}: 3411 (broad, —NH), 1712 (C═O); ^{1}H NMR (DMSO d_6, 400 MHz): δ 1.3 (t, 3H, –CH$_3$), δ 4.1 (q, 2H, —CH$_2$), δ 4.9 (s, 1H, —CH), δ 6.8–7.9 (m, 10H, Ar-H, and NH$_2$), δ 11.6 (s, 1H, —NH), δ 12.1 (s, 1H, —NH); ^{13}C NMR (DMSO d_6, 400 MHz): δ 14.5, 43.6, 54.3, 62.7, 63.8, 111.8, 114.2, 115.4, 116.7, 121.5, 124.5, 126.6, 127.8, 128.9, 131.6, 146.8, 153.6, 156.8, 159.3, 164.9, 172.5, 177.6; [M$^+$]: 547 and [M^{+2}]: 549.

2.12. Cytotoxicity assay

Three human cancer cell lines, i.e., MCF-7 (breast), A549 (lung) and Hela (cervical) cells, were used. Cell viability of these cancer cells in the presence of the novel phthalazinone based indole-pyran hybrids (**5a-j**) was assessed by using a colorimetric MTT assay (Sigma USA) (Mosmann 1983). The cancer cells were seeded in 100 µL of appropriate medium at a density of 2 × 10^5 cells and grown for 24 h in 96 well plate. This was followed by the addition of different concentrations of test compounds to the cells. After 48 hr incubation, each well was washed with PBS (200 µL) and then incubated with 10 % MTT solution for 2 h at 37 °C. Finally, a multimode reader was employed to determine the optical density of the solubilized formazan crystals at 570 nm (Tecan Infinite 200 PRO).

2.13. Molecular docking

The insilico analysis of the hybrids **5b** and **5h,** were executed using AutoDockTools 4.2 at the active site of human tankyrase-1 (Morris et al., 2009). The three-dimensional crystal structure of human tankyrase-1 was collected from RCSB (PDB ID: 7KKO) and used as the target protein. The protein molecule was processed by the removal of co-crystallized hetero molecules and water. The ChemDraw ultra 19.0 software was used to generate three-dimensional structures of active ligands **5b** and **5h**. Further, the energies were minimized using MOPAC (semiempirical quantum mechanics) with AM1

Table 1 Optimization of the four-component reaction with model substrates.[a]

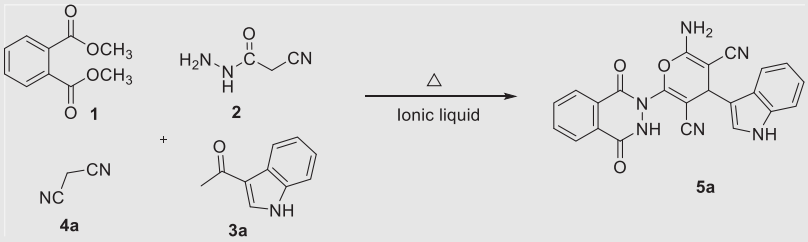

Entry	Ionic liquid	Temp (°C)	Time (min)	Yield % (5a)
1	[BMIM]Cl	75–80	240	78
2	[BMIM]Br	75–80	240	76
3	[BMIM]OH	75–80	90	80
4	[BMIM]BF$_4$	75–80	60	85
5	[BMIM]BF$_4$	65–70	360	82
6	[BMIM]BF$_4$	85–90	55	78
7	Ethanol	reflux	120	73
8	DMF	85–90	120	70
9	Water	85–90	180	68

[a] Reaction was carried out with 1 mmol of substrates **1,2,3a,4a**, and 8 mmol of ionic liquid.

MOZYME geometry acceleration. Around ten conformations were generated for each ligand and the best pose was selected with relatively lower binding free energy. The co-crystal ligand 09L (olaparib) was redocked with the target protein to validate the docking results. The 3D and 2D visualizations of the docked complexes were analyzed using PyMol and LIGPLOT, respectively (Wallace et al., 1995).

2.14. ADME and drug likeliness analysis

Computational analysis of ADME and drug-likeness properties of the synthesized hybrids (**5a-j**) were determined using SwissADME program provided by the Swiss Institute of Bioinformatics, Lausanne, Switzerland (Daina et al., 2017).

3. Results and discussion

3.1. Chemistry

To access the desired novel phthalazinone based indole-pyran hybrids **5a-j**, a new synthetic methodology was developed employing a one-pot four-component reaction promoted by an ionic liquid. We selected dimethyl phthalate **1** (1 mmol), 2-cyanoacetohydrazide **2** (1 mmol), 1H-indole-3-

Table 2 Optimization of the amount of $[BMIM]BF_4$.

Entry	$[BMIM]BF_4$ (mmol)	Temp./° C	Time (min)	Yield (5a%)
1	6	75–80	180	78
2	8	75–80	60	85
3	10	75–80	55	82

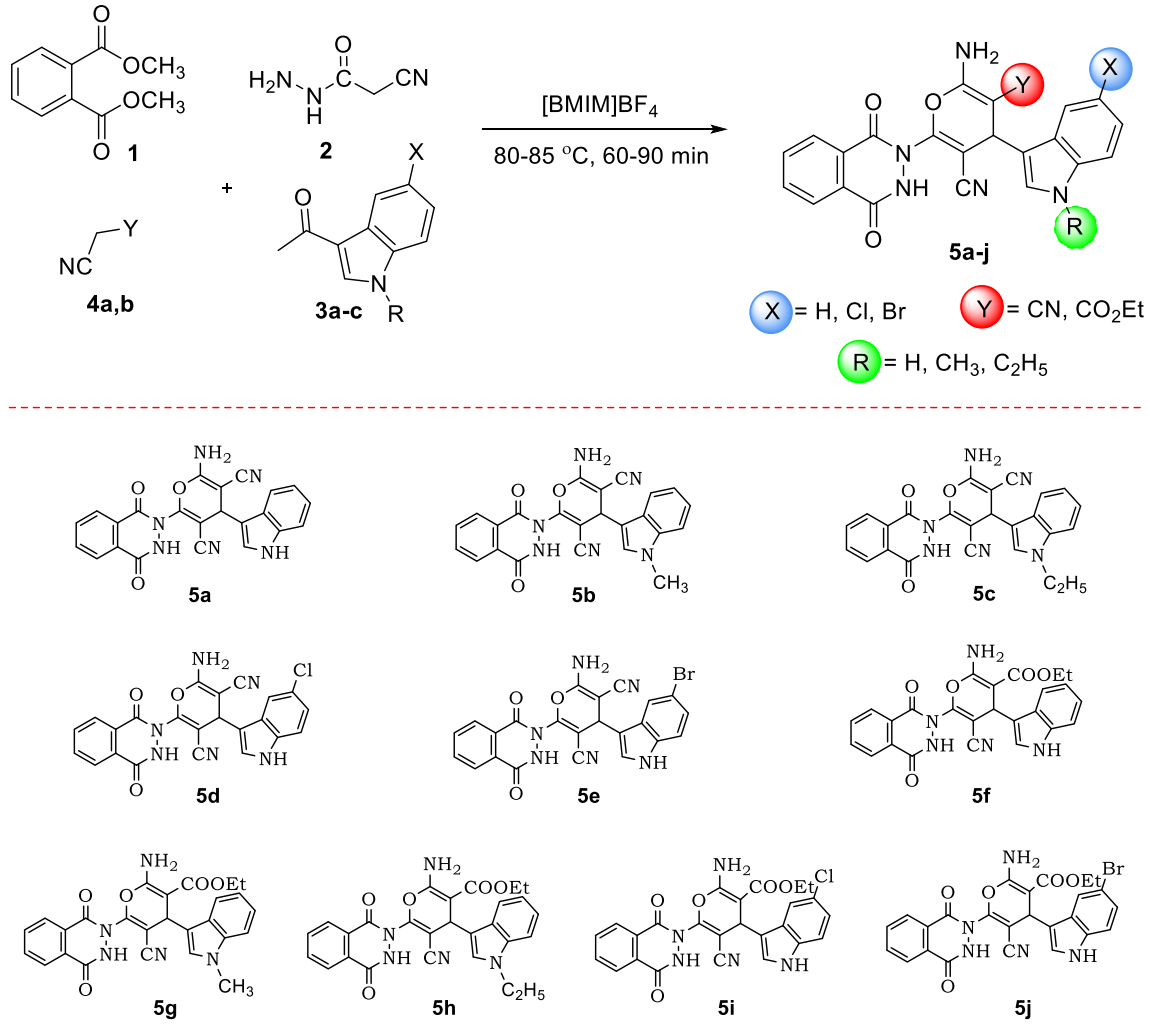

Scheme 1 Synthesis of novel phthalazinone based indole-pyran hybrids **5a-j.**

carbaldehydes **3a** (1 mmol), and malononitrile **4a** (1 mmol) as in the model multicomponent reaction. Initially, in this model reaction, different parameters such as the different ionic liquids, temperature, and amount of ionic liquid were screened to identify an optimized condition. The ionic liquids used in this study were based on 1-butyl-3-methyl imidazolium cation with diverse anions such as chloride [BMIM]Cl, fluoride [BMIM]F, hydroxide [BMIM]OH, and tetrafluoroborate [BMIM]BF_4. The screening of the different ionic liquids was carried around 75 °C, and the model MCR proceeded with good yields (76–78%) with halogen-based ionic liquids [BMIM]Cl and [BMIM]Br (Table 1). However, the reaction times were higher, i.e., 240 min (entries 1 and 2). With [BMIM]OH ionic liquid, the yields were slightly better with a significant reduction in the reaction time (90 min, entry 3). The best result was shown by [BMIM]BF_4 and the reaction proceeded with an 85 % yield with 60 min of reaction time (entry 4). As the temperature plays a critical role in reaction kinetics, we investigated the model reaction with [BMIM]BF_4 at both elevated and lowered temperatures. It was observed that on lowering the temperature, the reaction time increased substantially (entry 5). In contrast, the elevation of reaction temperature resulted in a decrease in reaction yield with a slight reduction in reaction time (entry 6). In addition to this, representative protic (ethanol) and aprotic (dimethylformamide) organic solvents were also investigated along with water. However, studied solvents showed lower yield and higher reaction time than ionic liquids (entry 7–9).

To further optimize the reaction conditions, the amount of ionic liquid was also investigated with different amounts of [BMIM]BF_4 at 75–80 °C (Table-2). It was observed that the multicomponent reaction achieved superior results with the use of 8 mmol [BMIM]BF_4 (Table 2).

Upon establishing the optimized reaction conditions, the methodology was extended by utilizing different indole derivatives (**3a-c**) and active methylene derivatives (**4a, b**) along with dimethyl phthalate **1** and 2-cyanoacetohydrazide **2** to access desired novel phthalazinone based indole-pyran hybrids **5a-j** (Scheme 1). The multicomponent reaction with various substrates afforded the corresponding products in good yields. The active methylene derivatives exhibited a slight effect on the yield of the reaction as malononitrile (**4a**) gave marginally higher yields when compared to ethyl 2-cyanoacetate (**4b**).

A plausible mechanism for the synthesis of hybrids **5a-j** mediated by ionic liquid is proposed. The ionic liquids with weakly basic tetrafluoroborate anion exhibit a weak base catalysis phenomenon (MacFarlane et al., 2006). It helps in the formation of a carbanion of **2**, which undertakes a nucleophilic attack on the carbonyl carbon of indole carboxaldehyde **3,**

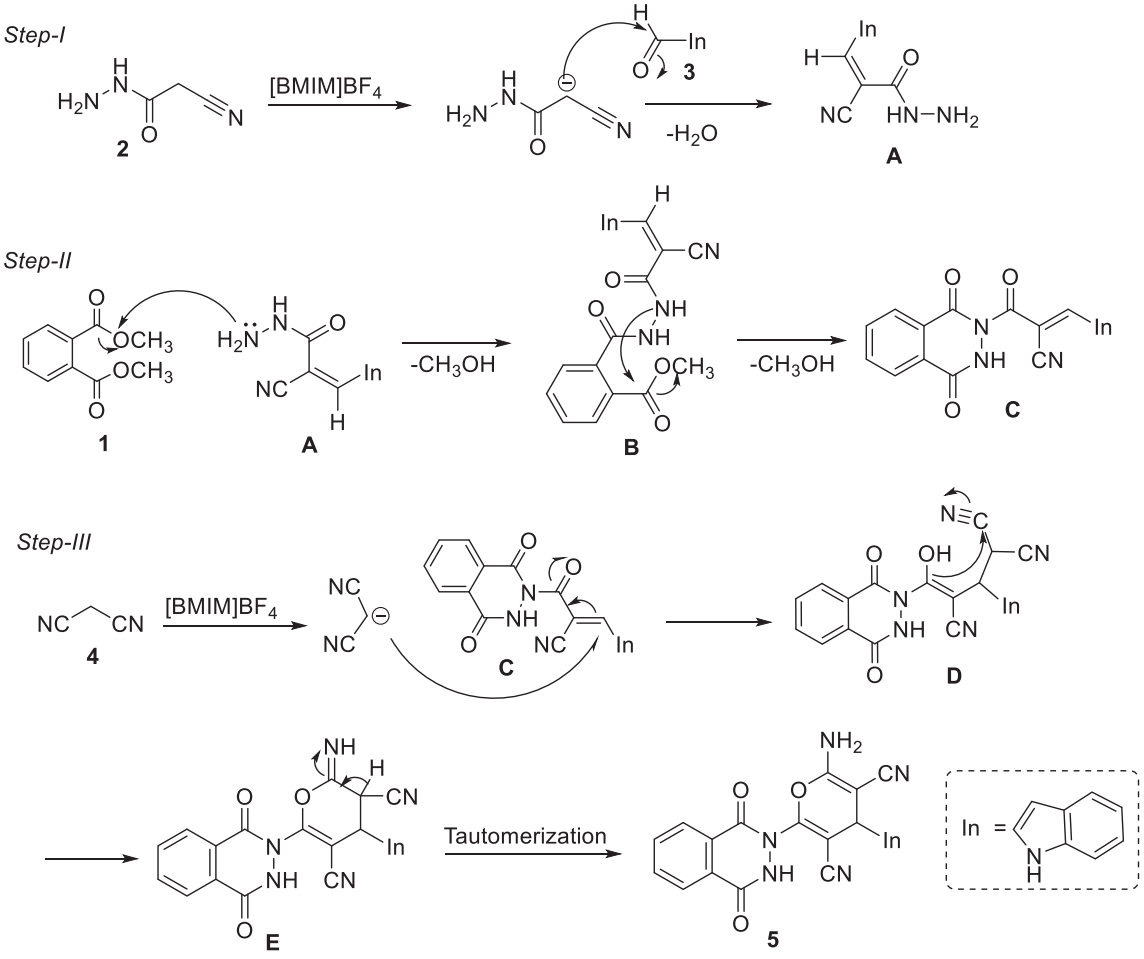

Fig. 2 Plausible mechanism for the formation of phthalazinone based indole-pyran hybrids **5a-j.**

affording the intermediate A. The intermediate A attacks dimethyl phthalate **1,** resulting in nucleophilic substitution to afford intermediate B, which loses a methanol molecule and forms intermediate C. A carbanion of malononitrile attacks the intermediate C to give intermediate D, which undergoes cyclization, affording imine intermediate E that tautomerizes to give the final product **5** (Fig. 2).

3.2. Anticancer activity

To assess the anticancer potency of the synthesized novel phthalazinone based indole-pyran hybrids **5a-j**, we conducted an MTT cytotoxicity assay against three cancer cell lines, namely, cervical (HeLa), lung (A549) and breast cancer (MCF-7) of human body. The synthesized hybrids exhibited good to moderate activity except for the hybrids, **5e** and **5j** (Table 3). Among the series, **5h** and **5b** were the most active hybrids with IC_{50}values of 5.8–9.6 μM against all the tested cells. Based on the screening results, hybrid **5h** was the most potent that unveiled significant activity against HeLa (IC_{50}: 5.8 μM) and MCF-7 (IC_{50}: 6.6 μM) cancer cell lines. Further, compounds **5a**, **5b,** and **5g** showed good activity towards all the tested cells with less than 15.0 μM of IC_{50} value. Similarly, the other compounds showed moderate cytotoxicity with all the cell lines that were screened.

The experimental data revealed an interesting structure–activity relationship (SAR) of the phthalazinone based indole-pyran hybrids (Table 3). The substitutions on the indole ring were crucial in imparting activity to the hybrids. The hybrids with *N*-methyl or ethyl substitution on the indole ring exhibited better activity than the hybrids with no substitution. On the other hand, the substitution on the 5th position of indole moiety with chlorine and bromine substituents reduced the activity, and the bromo derivatives showed complete loss of activity. Finally, no pronounced effect was noticed when the cyano group was replaced with ethoxycarbonyl group on the 5th position of the pyran ring. In our previous research finding, we reported the anticancer activity of pyran-linked phthalazinone-pyrazole derivatives. On comparing the present finding, it was observed the replacement of the pyrazole ring with a fused indole ring resulted in enhancement in cytotoxic potency of the hybrids. The most active compound of the present series **5h** was almost two folds more active than the active compound of phthalazinone-pyrazole series (Malik et al., 2021).

3.3. In silico binding studies

Tankyrases are members of poly ADP ribosyl polymerases (PARPs) enzymes that play a critical role in cell growth and

Table 3 Cytotoxic potency and structure–activity relationship of novel phthalazinone based indole-pyran hybrids **5a-j**.

Test compound	IC_{50} value in μM (Mean ± SD)[a]		
	MCF-7	**A549**	**HeLa**
5a	14.2 ± 0.36	11.2 ± 0.14	7.8 ± 0.19
5b	7.6 ± 0.22	6.6 ± 0.27	9.6 ± 0.15
5c	12.2 ± 0.18	> 100	11.4 ± 0.16
5d	24.7 ± 0.27	36.8 ± 0.25	19.3 ± 0.39
5e	> 100	100	> 100
5f	21.5 ± 0.32	16.6 ± 0.17	25.5 ± 0.38
5g	10.8 ± 0.14	12.2 ± 0.26	9.5 ± 0.23
5h	6.6 ± 0.12	9.3 ± 0.33	5.8 ± 0.16
5i	16.7 ± 0.26	14.5 ± 0.19	9.4 ± 0.44
5j	> 100	> 100	> 100
Doxorubicin	0.9 ± 0.06	0.7 ± 0.08	0.8 ± 0.09

[a] Results expressed as mean with standard deviation as experiments were performed in triplicates. Doxorubicin was used as a positive control for all the cell lines.

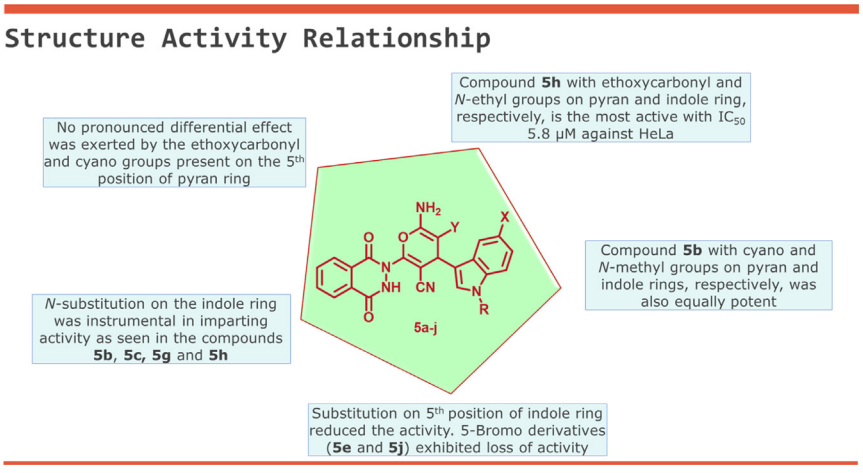

survival by interfering with Wnt/β-catenin signaling pathway (Haikarainen et al., 2014). The function of tankyrases is overdone in cancer cells resulting in their emergence as a novel molecular target in cancer disease (Lakshmi et al., 2017). Olaparib is reported to inhibit human tankyrase-1 protein, and the structural similarity of our novel phthalazinone based indole-pyran hybrids to olaparib encouraged us to perform in silico studies to recognize their binding affinity towards the mentioned protein. Based on the preliminary cytotoxicity results, the active hydrids **5b** and **5h** were studied for binding interactions with tankyrase-1 protein, and olaparib (09L) was the control. The studies revealed that both the docked ligands

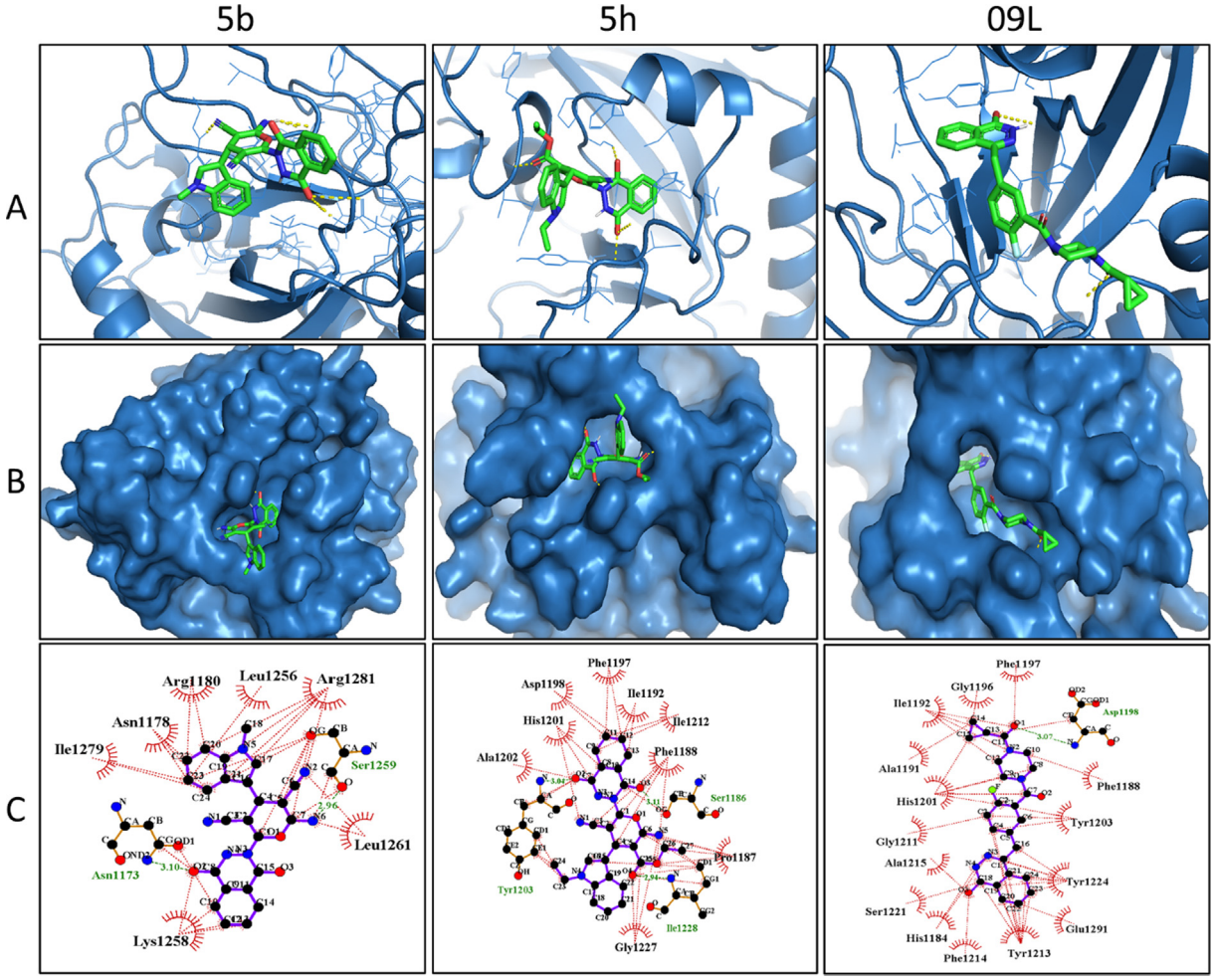

Fig. 3 (A) 3D binding conformations of the hybrids (**5b** and **5h**) with human tankyrase-1 protein (PDB ID: 7KKO) along with co-crystalized ligand (09L). (B) Surface representation of target protein with docked molecules at the binding site. (C) 2D binding interactions of the hydrids and olaparib with the target.

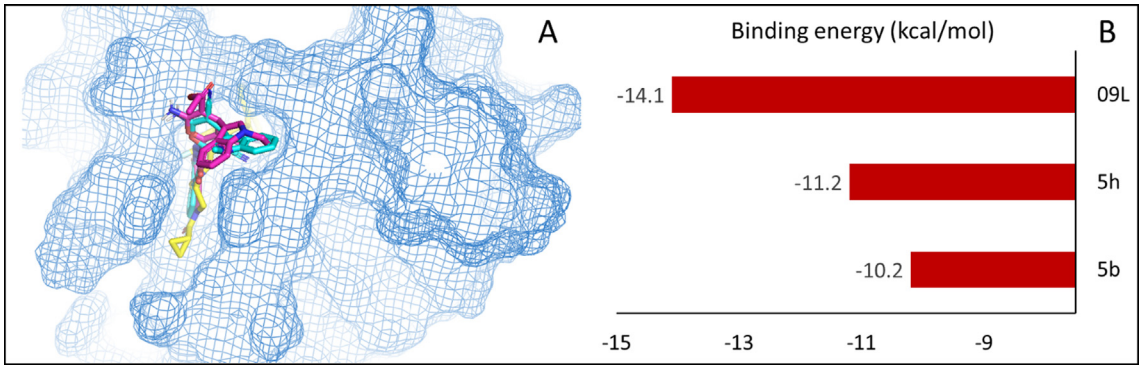

Fig. 4 (A) The overlayed structures of **5b** and **5h** along with co-crystalized ligand 09L at the binding site. (B) Binding energies (kcal/mol) shown was docked ligands at active site of human tankyrase-1 protein.

(**5b** and **5h**) displayed pronounced binding affinities towards the target receptor active site (Figs. 3 and 4). The hydrogen bond formation and hydrophobic interactions assisted in the binding of the ligands with the target protein. A set of ten different poses for each docked ligand was generated, and the best conformations were fully analyzed as shown in Fig. 3. The outcome of docking analysis revealed that **5b** and **5h** binded at the same site of the co-crystalized olaparib (09L) (Fig. 4A). The binding energy value provides a good indication of the affinity of a ligand towards the target receptor. The binding energy value of the active ligands **5b** was −10.2 Kcal/-mole, whereas the binding energy value of ligand **5h** was −11.2 Kcal/mol (Fig. 4B). The findings revealed that compound **5h** was the best-docked ligand as compared **5b**. The ligands **5b** and **5h** interacted via two hydrogen bond formation with the receptor protein compared to one hydrogen bond formation by the control (09L). However, the co-crystal ligand 09L exhibited more hydrophobic interaction and a higher binding energy score (−14.1 Kcal/mol). The different amino acid residues of the receptor protein responsible for various interactions with ligands **5b**, **5h** and 09L are provided (Table 4).

Table 4 Ligands interacting with different amino acid residues of the target.

Ligand	Protein–ligand interactions	
	H-bond	Hydrophobic bonds
5b	Asn1173, Ser1259	Leu1261, Lys1258, Ile1279, Asn1178, Arg1180, Leu1256, Arg1281
5h	Ser1186, Tyr1203	Pro1187, Phe1188, Ile1192, Phe1197, Asp1198, His1201, Ala1202, Gly1227, Ile1212
09L (Co-crystal ligand)	Asp1198	Phe1188, Tyr1203, Tyr1224, Glu1291, Tyr1213, Phe1214, his1184, Ser1221, Ala1215, Gly1211, His1201, Ala1191, Ile1192, Gly1196, Phe1197

3.4. ADME, drug likeness analyses

In drug design, computational pharmacodynamics and pharmacokinetics analysis help understand how the drug behaves in the physiological environment, thereby reducing drug attribution rate in advanced stages (Alqahtani 2017). The experimental results prompted us to carry out ADME and drug likeness calculations of our synthesized novel phthalazinone based indole-pyran hybrids **5a-j**. The cytochrome P450 (CYP) enzymes are responsible for the metabolism of foreign

Table 5 ADME predictions of phthalazinone based indole-pyran hybrids **5a-j**.

Compd	Inhibition of cytochrome enzymes					GI absorption	BBB permeation	log Kp (cm/s)	Bioactivity score
	CYP 1A2	CYP 2C19	CYP 2C9	CYP 2D6	CYP 3A4				
5a	N	Y	Y	N	N	Low	N	−7.31	0.55
5b	N	N	Y	N	Y	Low	N	−7.44	0.55
5c	N	Y	Y	Y	Y	Low	N	−7.30	0.55
5d	N	Y	Y	N	N	Low	N	−7.08	0.55
5e	N	Y	Y	N	N	Low	N	−7.31	0.55
5f	N	N	Y	N	N	Low	N	−7.25	0.11
5g	N	N	Y	N	Y	Low	N	−7.36	0.56
5h	N	N	Y	N	Y	Low	N	−7.23	0.56
5i	N	N	Y	N	N	Low	N	−7.01	0.11
5j	N	N	Y	N	N	Low	N	−7.23	0.11

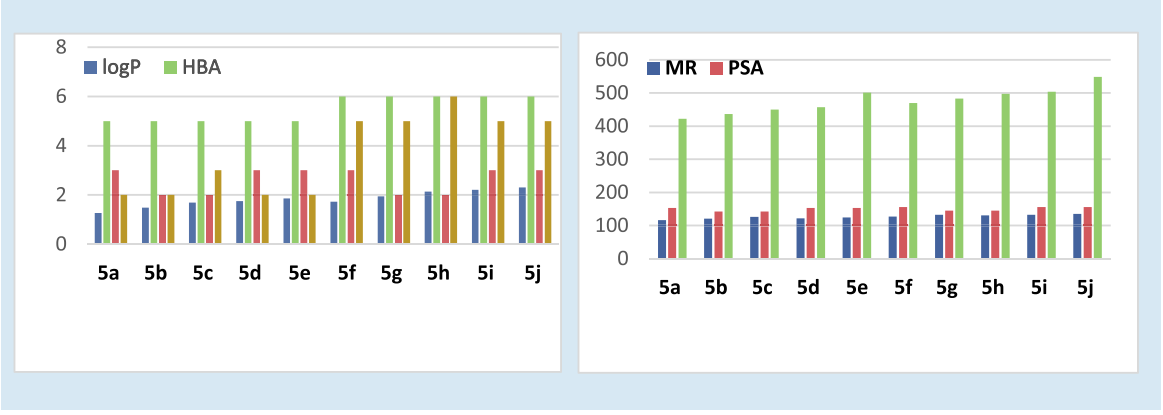

Fig. 5 Drug likeliness properties of hybrids **5a-j** where log P (lipophilicity), HBA (hydrogen bond acceptor), HBD (hydrogen bond donor), MW (molecular weight) denotes Lipinski filter. The descriptors RB (rotational bonds), MR (molecular refractivity), and PSA (polar surface area) denote additional drug likeliness filters.

substances in the body, and the inhibition of the five CYPs (CYPs 1A2, 2C19, 2C9, 2D6, and 3A4) results in significant drug-drug interactions that may lead to unanticipated adverse reactions (Beck et al. 2021). All the hybrids **5a-j** were shown to inhibit CYP2C9 isoenzyme with no inhibition of CYP1A2 isoform (Table 5). Interestingly, the most active hybrids **5h** and **5b** exhibited a similar cytochrome inhibition profile. In the absorption aspect, the hybrids **5a-j** were predicted to exhibit low gastrointestinal absorption properties and were non-permeable to the blood–brain barrier. The hybrids' skin permeability coefficient (log Kp) was in the range of −7.44 to −7.01 cm/s. In addition to this, the bioactivity score of the hybrids was around 0.55, except few of them (**5f**, **5i,** and **5j)** that showed a value of 0.11.

Drug likeliness predictions of the hybrids (**5a-j**) revealed that the Lipinski rule is followed by almost all the hybrids with respect to critical descriptors like molecular weight, lipophilicity (log P) number of hydrogen bond donors, and acceptors. In the case of hybrids **5e** and **5i**, the molecular weight was almost around the threshold of 500 amu, whereas a single Lipinski rule violation was shown by hybrid **5j** (Fig. 5). Some other additional descriptors related to Ghose and Veber's rules were also predicted. According to Ghose's rule, the molecular refractivity of a chemical compound in the range of 40–130 shows more drug likeliness properties. The hybrids **5a-5f** followed the rule with molecular refractivity value in the range of 116–127, whereas the other hybrids showed marginally higher molecular refractivity value (131–135). The number of rotational bonds (< 10) and topological surface area (< 140) are critical molecular descriptors according to Veber's rule. The computational analysis showed that the hybrids showed two to six rotational bonds. However, the TPSA values were slightly higher in the range of 142–156.

4. Conclusion

Cancer poses diverse challenges related to drug resistance and high incidence, thereby intensifying the need for new cancer drugs. Phthalazinone and indole moieties form the backbone of different FDA-approved medicines used in the treatment of cancer. We designed a series of ten novel phthalazinone based indole-pyran hybrids by employing a relatively safer synthetic protocol. After preliminary optimization studies, a one-pot multicomponent reaction mediated by [BMIM] BF_4 was developed to access the desired compounds. Cytotoxicity studies demonstrated that the hybrids **5b** and **5h** exhibited a single-digit IC_{50} in micromolar concentration against all the tested cancer cell lines. The SAR showed the *N*-substitution on indole ring with no substituents on the fifth position were critical for activity. Molecular docking at the active sites of the human tankyrase-1 protein revealed crucial interactions that resulted in a strong binding affinity towards the target protein. The hybrid **5h** exhibited more binding affinity than hybrid **5b**. Two hydrogen bond linkages were observed between both the hybrids and the different amino acid residues of the target protein. However, the hybrid **5h** showed nine hydrophobic interactions compared to seven exhibited by the hybrid **5b**. The ADME and drug likeliness analysis also provided valuable insights into the designed hybrids. A further structural tweaking and a detailed biological mechanistic study of the phthalazinone based indole-pyran hybrids could translate them into potential lead-like anticancer molecules.

Declaration of Competing Interest

The authors declare that they have no known competing financial interests or personal relationships that could have appeared to influence the work reported in this paper.

Acknowledgement

The authors would like to thank the Deanship of Scientific Research at Umm Al-Qura University for supporting this work by grant code 19-SCI-1-01-0019. The authors would like to extend their sincere appreciation to Taif University Researchers Supporting Project number (TURSP-2020/312), Taif University, Taif, Saudi Arabia.

Appendix A. Supplementary material

Supplementary data to this article can be found online at https://doi.org/10.1016/j.arabjc.2021.103560.

References

Alqahtani, S., 2017. In silico ADME-Tox modeling: progress and prospects. Expert Opin. Drug Metab. Toxicol. 13, 1147–1158. https://doi.org/10.1080/17425255.2017.1389897.

Arora, S., Balasubramaniam, S., Zhang, H., Berman, T., Narayan, P., Suzman, D., Bloomquist, E., Tang, S., Gong, Y., Sridhara, R., Turcu, F.R., Chatterjee, D., Saritas-Yildirim, B., Ghosh, S., Philip, R., Pathak, A., Gao, J.J., Amiri-Kordestani, L., Pazdur, R., Beaver, J.A., 2021. FDA approval summary: Olaparib monotherapy or in combination with bevacizumab for the maintenance treatment of patients with advanced ovarian cancer. Oncologist 26, e164–e172. https://doi.org/10.1002/onco.13551.

Banerjee, B., 2017. [Bmim]BF4: a versatile ionic liquid for the synthesis of diverse bioactive heterocycles. ChemistrySelect 2, 8362–8376. https://doi.org/10.1002/slct.201701700.

Beck, T.C., Beck, K.R., Morningstar, J., Benjamin, M.M., Norris, R. A., 2021. Descriptors of cytochrome inhibitors and useful machine learning based methods for the design of safer drugs. Pharmaceuticals (Basel). 14, 472. https://doi.org/10.3390/ph14050472.

Boussios, S., Abson, C., Moschetta, M., Rassy, E., Karathanasi, A., Bhat, T., Ghumman, F., Sheriff, M., Pavlidis, N., 2020. Poly (ADP-Ribose) polymerase inhibitors: Talazoparib in ovarian cancer and beyond. Drugs R D. 20, 55–73. https://doi.org/10.1007/s40268-020-00301-8.

Cioc, R.C., Ruijter, E., Orru, R.V.A., 2014. Multicomponent reactions: advanced tools for sustainable organic synthesis. Green Chem. 16, 2958–2975. https://doi.org/10.1039/C4GC00013G.

Dadashpour, S., Emami, S., 2018. Indole in the target-based design of anticancer agents: a versatile scaffold with diverse mechanisms. Eur. J. Med. Chem. 150, 9–29. https://doi.org/10.1016/j.ejmech.2018.02.065.

Daina, A., Michielin, O., Zoete, V., 2017. SwissADME: A free web tool to evaluate pharmacokinetics, drug-likeness and medicinal chemistry friendliness of small molecules. Sci. Rep. 7, 42717. https://doi.org/10.1038/srep42717.

Fleming, F.F., Yao, L., Ravikumar, P.C., Funk, L., Shook, B.C., 2010. Nitrile-containing pharmaceuticals: efficacious roles of the nitrile pharmacophore. J. Med. Chem. 53, 7902–7917. https://doi.org/10.1021/jm100762r.

Garnock-Jones, K.P., 2015. Panobinostat: First global approval. Drugs 75, 695–704. https://doi.org/10.1007/s40265-015-0388-8.

Gul, W., Hamann, M.T., 2005. Indole alkaloid marine natural products: an established source of cancer drug leads with considerable promise for the control of parasitic, neurological and other diseases. Life Sci. 78, 442–453. https://doi.org/10.1016/j.lfs.2005.09.007.

Haikarainen, T., Krauss, S., Lehtio, L., 2014. Tankyrases: structure, function and therapeutic implications in cancer. Curr. Pharm. Des. 20, 6472–6488. https://doi.org/10.2174/1381612820666140630101525.

Jampilek, J., 2019. Heterocycles in medicinal chemistry. Molecules (Basel, Switzerland) 24, 3839. https://doi.org/10.3390/molecules24213839.

Kumar, D., Sharma, P., Singh, H., Nepali, K., Gupta, G.K., Jain, S. K., Ntie-Kang, F., 2017. The value of pyrans as anticancer scaffolds in medicinal chemistry. RSC Adv. 7, 36977–36999. https://doi.org/10.1039/C7RA05441F.

Kumari, A., Singh, R.K., 2019. Medicinal chemistry of indole derivatives: current to future therapeutic prospectives. Bioorg. Chem. 89,. https://doi.org/10.1016/j.bioorg.2019.103021 103021.

Lakshmi, T.V., Bale, S., Khurana, A., Godugu, C., 2017. Tankyrase as a novel molecular target in cancer and fibrotic diseases. Curr. Drug. Targets. 18, 1214–1224. https://doi.org/10.2174/1389450117666160715152503.

Lei, Z., Chen, B., Koo, Y.-M., MacFarlane, D.R., 2017. Introduction: ionic liquids. Chem. Rev. 117, 663. https://doi.org/10.1021/acs.chemrev.7b00246.

MacFarlane, D.R., Pringle, J.M., Johansson, K.M., Forsyth, S.A., Forsyth, M., 2006. Lewis base ionic liquids. Chem. Commun. 18, 1905–1917. https://doi.org/10.1039/b516961p.

Malik, M.S., Asghar, B.H., Syed, R., Alsantali, R.I., Morad, M., Altass, H.M., Moussa, Z., Althagafi II, Jassas, R.S., Ahmed, S.A., 2021. Novel pyran-linked phthalazinone-pyrazole hybrids: synthesis, cytotoxicity evaluation, molecular modeling, and descriptor studies. Front. Chem. 9, 666573. https://doi.org/10.3389/fchem.2021.666573.

Morris, G.M., Huey, R., Lindstrom, W., Sanner, M.F., Belew, R.K., Goodsell, D.S., Olson, A.J., 2009. AutoDock4 and AutoDockTools4: automated docking with selective receptor flexibility. J. Comput. Chem. 30, 2785–2791. https://doi.org/10.1002/jcc.21256.

Mosmann, T., 1983. Rapid colorimetric assay for cellular growth and survival: application to proliferation and cytotoxicity assays. J. Immunol. Methods. 65, 55–63. https://doi.org/10.1016/0022-1759(83)90303-4.

Sangshetti, J., Pathan, S.K., Patil, R., Akber Ansari, S., Chhajed, S., Arote, R., Shinde, D.B., 2019. Synthesis and biological activity of structurally diverse phthalazine derivatives: a systematic review. Bioorg. Med. Chem. 27, 3979–3997. https://doi.org/10.1016/j.bmc.2019.07.050.

Shaheer Malik, M., Asghar, B.H., Azeeza, S., Obaid, R.J., Thagafi, I. I., Jassas, R.S., Altass, H.M., Morad, M., Moussa, Z., Ahmed, S. A., 2020. Facile Amberlyst A-21 catalyzed access of β-hydroxynitriles via epoxide opening in water. Arab. J. Chem. 13, 8200–8208. https://doi.org/10.1016/j.arabjc.2020.09.053.

Shirley, M., 2019. Rucaparib: a review in ovarian cancer. Target Oncol. 14, 237–246. https://doi.org/10.1007/s11523-019-00629-5.

Singh, T.P., Singh, O.M., 2018. Recent progress in biological activities of indole and indole alkaloids. Mini Rev. Med. Chem. 18, 9–25. https://doi.org/10.2174/1389557517666170807123201.

Sly, N., Gaspar, K., 2019. Midostaurin for the management of FLT3-mutated acute myeloid leukemia and advanced systemic mastocytosis. Am. J. Health Syst. Pharm. 76, 268–274. https://doi.org/10.1093/ajhp/zxy050.

Vekariya, R.L., 2017. A review of ionic liquids: applications towards catalytic organic transformations. J. Mol. Liq. 227, 44–60. https://doi.org/10.1016/j.molliq.2016.11.123.

Vila, N., Besada, P., Costas, T., Costas-Lago, M.C., Terán, C., 2015. Phthalazin-1(2H)-one as a remarkable scaffold in drug discovery. Eur. J. Med. Chem. 97, 462–482. https://doi.org/10.1016/j.ejmech.2014.11.043.

Walker, D.K., Jones, R.M., Nedderman, A.N.R., Wright, P.A., 2010. Primary, secondary and tertiary amines and their isosteres. metabolism, pharmacokinetics and toxicity of functional groups: impact of chemical building blocks on ADMET. Roy. Soc. Chem., 168–209 https://doi.org/10.1039/9781849731102-00168. Chapter 4.

Wallace, A.C., Laskowski, R.A., Thornton, J.M., 1995. LIGPLOT: a program to generate schematic diagrams of protein-ligand interactions. Protein Eng. 8, 127–134. https://doi.org/10.1093/protein/8.2.127.

Zaib, S., Khan, I., 2020. Synthetic and medicinal chemistry of phthalazines: recent developments, opportunities and challenges. Bioorg. Chem. 105,. https://doi.org/10.1016/j.bioorg.2020.104425 104425.